ELSEVIER

Journal of Alloys and Compounds 408–412 (2006) 831–834

Journal of ALLOYS AND COMPOUNDS

www.elsevier.com/locate/jallcom

Direct observation of the spatial distribution of samarium ions in alumina–silica macroporous monoliths by laser scanning confocal microscopy

Shunsuke Murai, Koji Fujita *, Kazuki Nakanishi, Kazuyuki Hirao

Department of Material Chemistry, Graduate School of Engineering, Kyoto University, Nishikyo-ku, Kyoto 615-8510, Japan

Received 2 August 2004; received in revised form 17 December 2004; accepted 13 January 2005
Available online 31 May 2005

Abstract

We have investigated the spatial distribution of Sm^{2+} inside macroporous alumina–silica (Al_2O_3–SiO_2) glasses having three-dimensionally interconnected skeletons. The Sm^{2+}-doped Al_2O_3–SiO_2 glasses are prepared via an alkoxy-derived sol–gel route in the presence of poly (ethylene oxide) and $SmCl_3{\cdot}6H_2O$. The well-defined macroporous morphology is obtained by the concurrence of the phase separation and the sol–gel transition. The reduction of Sm^{3+} to Sm^{2+} is accomplished by heat treatment under a reducing atmosphere. Two-dimensional images of the fluorescence due to the 4f–4f transition of Sm^{2+} with the aid of a laser scanning confocal microscope reveal the spatially uniform dispersion of Sm^{2+} inside the Al_2O_3–SiO_2 skeleton.

Keywords: Sol–gel method; Phase separation; Porous material; Samarium ion; Multiple light scattering; Laser scanning confocal microscopy

1. Introduction

Light transportation in dielectrically disordered media is modified by multiple scattering. In strongly scattering media where the indices of refraction vary on the length scale comparable to the wavelength of light, interference of multiple-scattered light leads to various remarkable phenomena such as photon localization [1]. Recently, a novel optical memory effect was observed in strongly scattering media doped with Sm^{2+} [2–4]. Irradiation of the scattering medium with a monochromatic light creates a three-dimensional interference pattern of multiple-scattered light within the medium. By recording the interference pattern through photobleaching of Sm^{2+}, the information on the wavelength and wave-vector of the writing beam is stored in the form of spatial distribution of the light intensity. Optical paths inside the scattering medium are affected by absorption and scattering, and thus it is important to control both parameters. So far, multiple-scattering hosts offered for this optical memory effect have been limited to compacted powders, including aggregates of semiconductor nanoparticles, and ground glasses [2–4]. The control of the scattering strength is performed by changing the size of particles, while the amount of absorption is tuned by Sm^{2+} concentration.

In order to obtain spatially disordered dielectrics with tunable scattering strength, we have focused on macroporous monoliths instead of conventional powder-based disordered systems [5–7]. Compared to powder-based systems, our monoliths are advantageous in terms of the strict control of scattering strength through the precise morphology control. The sol–gel-derived macroporous structure is formed when the transient structure of phase separation developed during hydrolysis and condensation of metal alkoxides is chemically frozen by the sol–gel transition [8,9]. The sizes of pores and skeletons can be precisely controlled by the relative rate of phase separation to that of sol–gel transition; the pore diameter can be varied from submicron to several tens of micrometers while keeping the sharp pore size distribution. This feasibility allows us to tune the scattering strength

* Corresponding author. Tel.: +81 75 383 2432; fax: +81 75 383 2420.
E-mail address: fujita@sung7.kuic.kyoto-u.ac.jp (K. Fujita).

0925-8388/$ – see front matter © 2005 Elsevier B.V. All rights reserved.
doi:10.1016/j.jallcom.2005.01.085

systematically. The macroporous monoliths, if combined with photoreactive ions such as Sm^{2+}, would be regarded as new materials for the scattering-based optical memory effect.

In our previous study, we demonstrated the successful preparation of Sm^{2+}-doped aluminosilicate monoliths with interconnected macropores by the sol–gel method including the phase separation [10,11]. The alumina–silica (Al_2O_3–SiO_2) system was selected as the host for Sm^{2+} because the presence of Al^{3+} was effective in reducing Sm^{3+} to Sm^{2+} during the heat treatment under reducing atmosphere [12–14]. This result is in contrast to that in pure silica glass, where samarium ions tend to be present as the trivalent state even after the heat treatment in reducing conditions. In this study, we have observed two-dimensional fluorescence images of Sm^{2+} in macroporous Al_2O_3–SiO_2 monoliths using a laser scanning confocal microscope (LSCM) in order to obtain information about the spatial distribution of Sm^{2+} inside the interconnected skeleton. We show that Sm^{2+} ions are spatially homogeneously distributed inside the skeleton.

2. Experimental details

Tetramethoxysilane, $Si(OCH_3)_4$ (Shin-Etsu Chemical Co., Japan) and aluminum *sec*-butoxide, $Al(OC_4H_9)_3$ (Tokyo-kasei, Japan) were used without purification. For the purpose of lowering the viscosity, $Al(OC_4H_9)_3$ was mixed with *sec*-butanol with a volume ratio of 1:2. Samarium ion was provided in the form of $SmCl_3{\cdot}6H_2O$ (Mitsuwa's Pure Chemical, Japan). Poly(ethylene oxide), PEO, with average molecular weight of 100,000 (Aldrich, USA) was used as a polymer component to induce phase separation, and nitric acid as a catalyst for hydrolysis and condensation of metal alkoxides. The starting composition listed in Table 1 was determined to obtain the glass having the nominal composition of $10AlO_{3/2}{\cdot}90SiO_2{\cdot}1SmO$ (mol%).

Gels were prepared as reported elsewhere [10,11]. First, PEO was dissolved in 2 M nitric acid aqueous solution (10 ml) in the presence of $SmCl_3{\cdot}6H_2O$, and the solution was held in an ice bath. Separately, $Si(OCH_3)_4$ was added to the mixture of $Al(OC_4H_9)_3$ and *sec*-butanol at room temperature, and stirred vigorously to yield a homogeneous solution. The aqueous solution of PEO was finally mixed with the alkoxide mixture, and stirred vigorously for 30 min. The resultant transparent solution was poured into a glass container, which was sealed and kept at 60 °C for gelation. After gelation, the wet gel was aged for 24 h, and dried at 60 °C to evaporate the solvent. The resultant gel is referred to as dried gel. The dried gels were calcined at 500 °C for 2 h in air to remove PEO. For the conversion of Sm^{3+} into Sm^{2+}, the calcined gel containing Sm^{3+} was heat-treated at 1000 °C for 10 h under flow of a reducing gas of 50 vol% N_2, 47.5 vol% Ar, and 2.5 vol% H_2. Hereafter, the sample heat-treated in the reducing gas is denoted as the reduced sample. To clarify the effect of heat treatment in the reducing gas on the valence state of samarium ions, we also prepared the sintered sample by heating the calcined gel at 1000 °C for 10 h in air.

Table 1
Starting composition of the sample (unit: g)

60% $HNO_{3\,aq}$	2.10
H_2O	8.48
$Si(OCH_3)_4$	4.64
$Al(OC_4H_9)_3$	0.83
sec-butanol	1.39
PEO	0.80
$SmCl_3{\cdot}6H_2O$	0.13

A scanning electron microscope (SEM; S-2600N, Hitachi Ltd., Japan) was used to observe the macroscopic morphology of the samples. Fluorescence spectra were measured at room temperature with a fluorescence spectrophotometer (Hitachi-850) using a 488 nm line of an Ar^+ laser as the excitation light. Two-dimensional image of fluorescence was taken using a LSCM (LSM5 Pascal, Carl Zeiss) with an oil-immersed 63× objective lens (Plan-Apochromat, numerical aperture = 1.4, Carl Zeiss) in order to examine the spatial distribution of samarium ions in the skeleton of macroporous monoliths. For the LSCM observation, the macroporous samples were immersed in a mixture of chloroform (refractive index, $n_D^{20} = 1.447$) and toluene ($n_D^{20} = 1.497$) with a volume ratio of 68:32, which had a refractive index of ∼1.46. Since the mixture had the same refractive index as that of the samples, the immersed sample became transparent, allowing the laser light to transmit through the turbid sample. An Ar^+ laser with a wavelength of 488 nm was used to excite the immersed sample. The fluorescence emitted from the samples was selectively detected through a colored glass filter which cut the light waves shorter than 505 nm. A pinhole in front of the detector effectively excludes out-of-focus light, enhancing the depth resolution.

3. Results and discussion

Fig. 1 depicts the micrometer-range morphology for dried and heat-treated samples. Fig. 1(a) is the SEM image for dried gel, which exhibits the bicontinuous morphology of gel skeletons and pores. The bicontinuous morphology is formed by the concurrence of phase separation and sol–gel transition. In the reaction solution, parallel to the hydrolysis and condensation of metal alkoxides, a spinodal-type phase separation is induced by the adsorption of PEO on the surface of alkoxy-derived oligomers. The PEO-adsorbed surface of oligomers becomes hydrophobic, and repulsively interacts with the solvents. As a result, the initially homogeneous solution separates into gel- and solvent-rich phases [15]. The sol–gel transition to fix the transient structures of phase separation and the subsequent solvent evaporation yield the macroporous structure possessing three-dimensionally interconnected gel skeletons (Fig. 1(a)). The pore diameter of the present sample is about 3–4 μm. The size and volume fraction of micrometer-sized pores can be precisely controlled by the starting com-

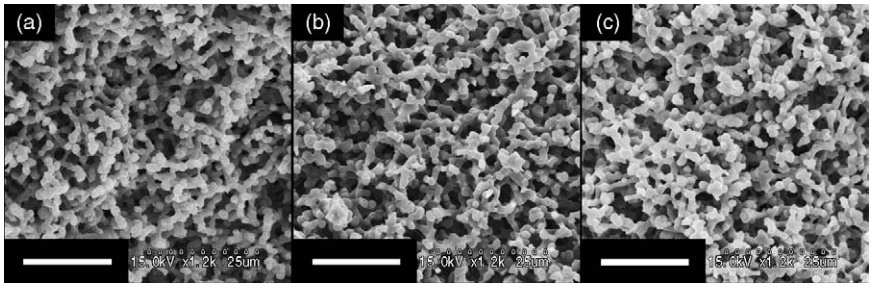

Fig. 1. SEM images for the dried (a), sintered (b), and reduced samples (c). Bars = 20 μm.

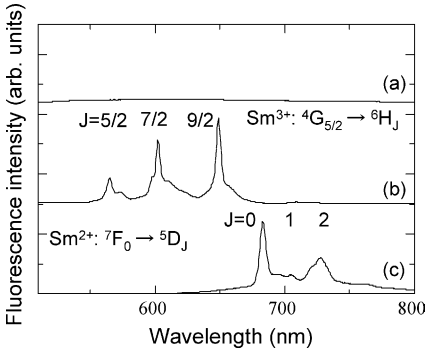

Fig. 2. Fluorescence spectra for the dried (a), sintered (b), and reduced samples (c). The amplitude of the spectrum denoted as (a) is scaled up by a factor of 50.

position [11]. The SEM images for the sintered and reduced samples are displayed in Fig. 1(b) and (c), respectively. The macroporous morphology is retained even after heat treatment.

Room-temperature fluorescence spectra are shown in Fig. 2 for the dried gel and sintered and reduced samples. Fig. 2(a) corresponds to the fluorescence spectrum for the dried gel. No emission peaks ascribed to electronic transitions of Sm^{3+} or Sm^{2+} are detected. This can be mainly related to a multiphonon relaxation process by which the excited electronic states of samarium ions decay nonradiatively by exciting lattice vibrations [16]. In the dried gel, there still remain many unreacted OH groups attached to silicon or aluminium. The phonon energies of OH group ($\sim$3400 cm^{-1}) [17] is higher than those of Al–O ($\sim$800 cm^{-1}) [18] and Si–O bonds ($\sim$1000 cm^{-1}) [19]. Since higher phonon energy contributes to the multiphonon relaxation process, the presence of OH groups surrounding samarium ions leads to the quenching of emission. Fig. 2(b) and (c) represents fluorescence spectra for the sintered and reduced samples, respectively. In Fig. 2(b), the emission peaks ascribed to the 4f–4f transitions of Sm^{3+} are observed; the emission lines at around 565, 603, and 649 nm are assigned to the $^4G_{5/2} \rightarrow {}^6H_{5/2,\,7/2,\,9/2}$ transitions of Sm^{3+}, respectively [20]. On the other hand, new emission peaks appear in the reduced sample (Fig. 2(c)). The peaks observed at around 684, 700, and 728 nm are assigned to the 4f–4f transitions of Sm^{2+}, corresponding to the $^5D_0 \rightarrow {}^7F_{0,\,1,\,2}$ transitions of Sm^{2+}, respectively [20]. The application of heat treatments promotes dehydroxylation of the gel skeleton to form Si–O–Si and Si–O–Al bonds, leading to the intense emission through the reduction of the probability of multiphonon decay. The comparison between Fig. 2(b) and (c) confirms that Sm^{3+} is converted to Sm^{2+} in aluminosilicate glasses by the heat treatment in reducing atmosphere [12,13].

Two-dimensional fluorescence LSCM images are shown in Fig. 3 for the dried gel and sintered and reduced samples. Fig. 3(a) displays the LSCM image for the dried gel. It is found that the contrast in brightness reflects the skeleton geometry of the dried gel (Fig. 1(a)), although no emission peaks are detected in the conventional fluorescence spectrum for the same gel (see Fig. 2(a)). It should be noted that any bright contrast was not observed in the fluorescence LSCM image for the dried gel prepared from the solution without $SmCl_3{\cdot}6H_2O$, implying the absence of emission lines detectable through LSCM. Therefore, we tentatively assign the fluorescence observed for the samarium-doped dried gel to the samarium-related centers. Fig. 3(b) and (c) corresponds to the fluorescence LSCM images for the sintered and reduced

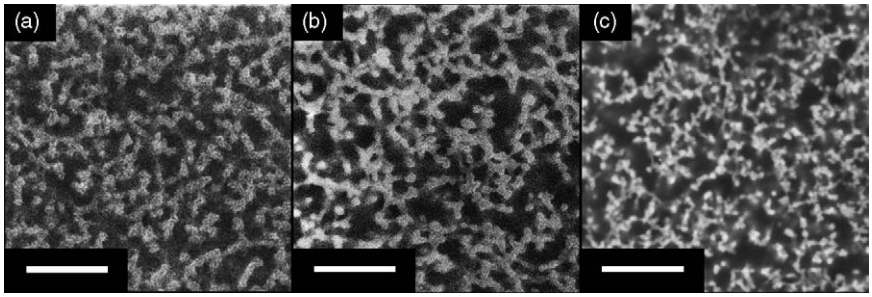

Fig. 3. Two-dimensional fluorescence LSCM images for the dried (a), sintered (b), and reduced samples (c). Bars = 20 μm.

samples, respectively. Judging from the fluorescence spectra in Fig. 2(b) and (c), these bright contrasts are caused by the emission lines due to the 4f–4f transitions of Sm^{3+} and Sm^{2+}, respectively. The comparison of Figs. 1 and 3 reveals that the bright area reflects the overall structure of Al_2O_3–SiO_2 skeleton, indicating the spatially homogeneous dispersion of samarium ions inside the skeleton. Here, it should be noted that the spatial distribution of the fluorescence is sensitive to the heat-treatment condition. For example, when the sintering time is relatively short, the fluorescence in the vicinity of skeleton surface tends to be more intense than that inside the skeleton. Although the detailed mechanism is not fully elucidated yet, the inhomogeneity may be caused by the insufficient diffusion of samarium ions during the sintering process.

As mentioned above, scattering-based optical memory effect depends strongly on the amounts of optical absorption and optical scattering [2–4]. Our previous study showed that the sol–gel method including phase separation can provide a series of macroporous monoliths with varied scattering strength through a systematic morphology control [5]. In this study, we also confirmed the homogeneous incorporation of Sm^{2+} into the Al_2O_3–SiO_2 skeleton, which eliminates the possibility that the Sm^{2+} ions are only adsorbed on the surface of the skeleton. Namely, our approach enables the uniform dispersion of Sm^{2+} as well as the precise morphology control, allowing the preparation of photoreactive macroporous monoliths with controlled scattering strength. Such optically active macroporous materials are difficult to be fabricated by other methods. For example, rare-earth-doped macroporous silicate glasses could not be obtained using a conventional technique involving heat-treatment-induced phase separation of melt-quenched glasses and the subsequent acid treatment. In this scheme, rare-earth ions are leached out during the acid-treatment [10]. The preparation principle presented here gives a simple route to obtain Sm^{2+}-doped macroporous monoliths, which are really applicable to the optical memory effect based on the interference of multiple-scattered light.

4. Conclusions

We have demonstrated the successful fabrication of macroporous $10AlO_{3/2}{\cdot}90SiO_2$ (mol%) glasses doped with samarium ions utilizing the sol–gel process including the phase separation, and clarified the macroscopic spatial distribution of samarium ions inside the skeleton by means of two-dimensional fluorescence LSCM observation. The interconnected macropores are formed when the phase separation and sol–gel transition concur to fix the transient structure of phase separation. The conversion of Sm^{3+} to Sm^{2+} is achieved through the heat treatment under a reducing atmosphere. Fluorescence LSCM images prove that the spatial distribution of samarium ions inside the skeleton is rather uniform at the stage of dried gel and that the macroscopically homogeneous dispersion of samarium ions is maintained even after heat treatment at 1000 °C.

Acknowledgements

This work is financially supported by the Industrial Technology Research Grant Program (’04A24023) from New Energy and Industrial Technology Development Organization (NEDO) of Japan, the Grant-in-Aid for Young Scientists from the Ministry of Education, Culture, Sports, Science and Technology (MEXT) of Japan, and the Asahi Glass Foundation. The first author (S.M.) is grateful to the Fellows of the Japan Society for the Promotion of Science (JSPS).

References

[1] C.M. Soukoulis (Ed.), Photonic Crystals and Light Localization in the 21st Century, Kluwer, Dordrecht, 2001.
[2] A. Kurita, Y. Kanematsu, M. Watanabe, K. Hirata, T. Kushida, Phys. Rev. Lett. 83 (1999) 1582.
[3] A. Kurita, Y. Kanematsu, M. Watanabe, K. Hirata, T. Kushida, J. Lumin. 87–89 (2000) 986.
[4] K. Fujita, Y. Ohashi, K. Hirao, Opt. Lett. 28 (2003) 567.
[5] S. Murai, K. Fujita, K. Nakanishi, K. Hirao, J. Appl. Phys. Jpn. 43 (2004) 5359.
[6] S. Murai, K. Fujita, K. Nakanishi, K. Hirao, J. Non-Cryst. Solids 345–346 (2004) 438.
[7] K. Fujita, J. Konishi, K. Nakanishi, K. Hirao, Appl. Phys. Lett. 85 (2004) 5595.
[8] K. Nakanishi, N. Soga, J. Am. Ceram. Soc. 74 (1991) 2518.
[9] K. Nakanishi, J. Porous Mater. 4 (1997) 67.
[10] K. Fujita, S. Murai, Y. Ohashi, K. Nakanishi, K. Hirao, Chem. Lett. 33 (2004) 1120.
[11] S. Murai, K. Fujita, K. Nakanishi, K. Hirao, J. Phys. Chem. B 43 (2004) 16670.
[12] M. Nogami, Y. Abe, J. Appl. Phys. 81 (1997) 6351.
[13] M. Nogami, Y. Abe, Phys. Rev. B 56 (1997) 182.
[14] K. Fujita, K. Nouchi, K. Hirao, J. Lumin. 86 (2000) 305.
[15] K. Nakanishi, H. Komura, R. Takahashi, N. Soga, Bull. Chem. Soc. Jpn. 67 (1994) 1327.
[16] T. Miyakawa, D.L. Dexter, Phys. Rev. B 1 (1970) 2961.
[17] A. Martucci, A. Chiasera, M. Montagna, M. Ferrari, J. Non-Cryst. Solids 322 (2003) 295.
[18] S. Tanabe, T. Ohyagi, T. Hanada, N. Soga, J. Ceram. Soc. Jpn. 101 (1993) 78.
[19] S. Todoroki, S. Tanabe, K. Hirao, N. Soga, J. Non-Cryst. Solids 136 (1991) 213.
[20] D.H. Dho, K. Hirao, N. Soga, M. Nogami, J. Non-Cryst. Solids 215 (1997) 192.